Local Structure of Multiferroic MnWO$_4$ and Mn$_{0.7}$Co$_{0.3}$WO$_4$ Revealed by the Evolutionary Algorithm

JANIS TIMOSHENKO,* ANDRIS ANSPOKS, ALEKSANDR KALINKO, INGA JONANE, AND ALEXEI KUZMIN

Institute of Solid State Physics, University of Latvia, Latvia

A novel reverse Monte Carlo/evolutionary algorithm scheme was applied to the analysis of the W L$_3$-edge and Mn(Co) K-edges EXAFS spectra from multiferroic MnWO$_4$ and Mn$_{0.7}$Co$_{0.3}$WO$_4$. A 3D structural model, consistent with the experimental data, was obtained, and the influence of composition and temperature on the local structure of tungstates is discussed.

Introduction

Manganese tungstate MnWO$_4$ is a multiferroic material with wolframite-type structure, which exhibits a ferroelectric polarization in the antiferromagnetically ordered incommensurate state AF2, existing in the temperature range between 8 K and 12.3 K [1]. Below 8 K the magnetic ordering of MnWO$_4$ becomes a collinear commensurate AF1, whereas a sinusoidal incommensurate magnetic structure AF3 exists between 12.3 K and 13.5 K and transits to the paramagnetic phase above 13.5 K [1]. It is known that the addition of Co atoms allows one to tune the magnetic properties of MnWO$_4$ [2]. However, the relation between the multiferroic properties of Mn$_{1-c}$Co$_c$WO$_4$ and its structure is still debatable.

Recently we have addressed this question using the W L$_3$-edge and Mn(Co) K-edge extended X-ray absorption fine structure (EXAFS) spectroscopy [3]. However, the conventional EXAFS data analysis does not allow one to extract information beyond the first coordination shell due to the complex structure of the material. Therefore in this study we report on the results of the local structure reconstruction in MnWO$_4$ and Mn$_{0.7}$Co$_{0.3}$WO$_4$ using the advanced approach based on reverse Monte Carlo (RMC) and evolutionary algorithm (EA) techniques [4]. An important part of our RMC/EA implementation is the wavelet transform (WT) [5, 6].

Experimental Data and Wavelet Analysis

$MnWO_4$ and $Mn_{0.7}Co_{0.3}WO_4$ powders were synthesized using the co-precipitation technique [3]. The W L_3-edge and Mn(Co) K-edges EXAFS spectra were acquired in transmission mode at the HASYLAB/DESY C bending-magnet beamline [7]. Sample temperature was controlled in the range from 6 K to 300 K using helium-flow cryostat.

The experimental EXAFS spectra, obtained after conventional data reduction [8], are compared in Fig. 1. Their low-frequency component, well visible in the k-space range up to 6 $\overset{\circ}{A}^{-1}$, corresponds to the contribution from the first coordination shell (six oxygen atoms) around absorbing metal atom (W, Mn or Co). The most pronounced changes in this region are observed at the Mn K-edge in $Mn_{0.7}Co_{0.3}WO_4$: the amplitude of EXAFS increases, indicating that MnO_6 octahedra are getting less distorted with respect to the case of pure $MnWO_4$, as reported in [3].

The high-frequency part of EXAFS spectra is mainly due to contributions from outer coordination shells, which can be conveniently separated using the wavelet transform [5, 6]. Comparing wavelet images (Fig. 2), one can conclude that this part of EXAFS is dominated by the Mn-W and Co-W contributions. Unlike the contribution from the first coordination shell, this component of EXAFS is sensitive to temperature effects and the presence of Co atoms. To analyze it quantitatively, we employ our RMC/EA simulation scheme.

RMC/EA Simulations

RMC method [9, 10] allows one to analyze EXAFS data taking into account the influence of multiple-scattering (MS) effects and outer coordination shells, as well as structural and thermal disorder. In this approach, a 3D structure model is constructed and atomic coordinates are changed in a random iterative process, aimed to minimize the difference between the experimental and configuration-averaged (CA) EXAFS spectra. The theoretical CA-EXAFS is calculated at each iteration using the ab-initio real-space MS FEFF8 code [11] for the given structure model. The implementation of evolutionary algorithm (EA) in the conventional RMC scheme improves the convergence properties
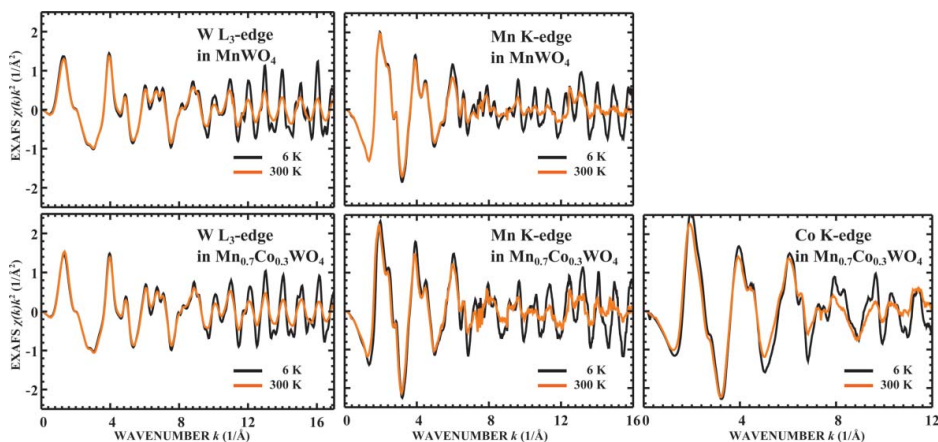

Figure 1. The experimental W L_3-edge (left panels) and Mn(Co) K-edges EXAFS spectra (middle and right panels) for $Mn_cCo_{1-c}WO_4$ ($c = 1.0$ and 0.7) at $T = 6$ and 300 K.
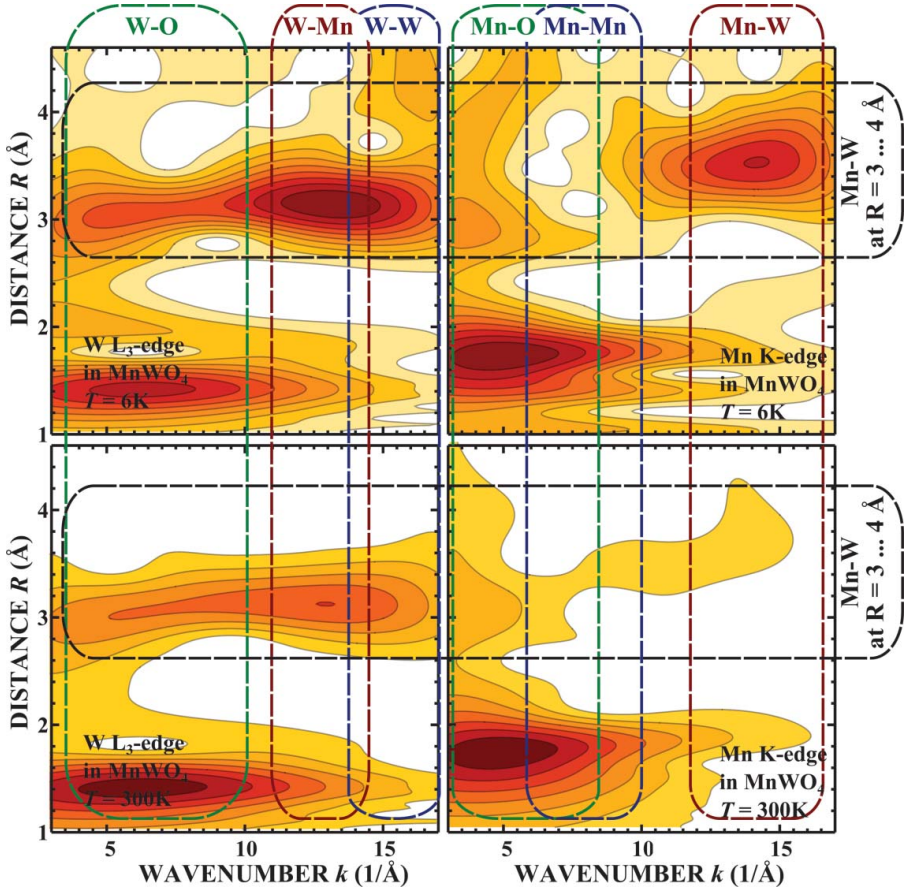
Figure 2. Wavelet analysis of the W L$_3$ (left panels) and Mn K-edge EXAFS spectra (right panels) for MnWO$_4$ at $T = 6$ and 300 K.

of simulations and makes feasible the analysis of EXAFS spectra for complex materials [4, 12].

In this study RMC/EA calculations were used to construct structural models that correspond simultaneously to the experimental W L$_3$-edge and Mn(Co) K-edges EXAFS spectra. As it was demonstrated in our recent paper [12], the simultaneous fitting of EXAFS at several absorption edges is required to obtain unambiguous solution for such complex materials as tungstates.

Crystalline MnWO$_4$ and Mn$_{0.7}$Co$_{0.3}$WO$_4$ were modeled as infinite crystals employing periodic boundary conditions for supercell, containing $4 \times 4 \times 4$ unit cells of corresponding tungstate. The values of lattice parameters were taken from the diffraction experiment [13]. In the simulations for Mn$_{0.7}$Co$_{0.3}$WO$_4$ the sites, occupied by Co atoms, were selected randomly before RMC/EA calculations, and for each temperature point simulations were repeated ten times with different distributions of Co atoms.

MS contributions were accounted up to the 4th order. A comparison of the experimental and calculated EXAFS spectra was carried out using WT in k and R spaces, as shown in Fig. 3. The structure models, obtained from RMC/EA calculations, describe
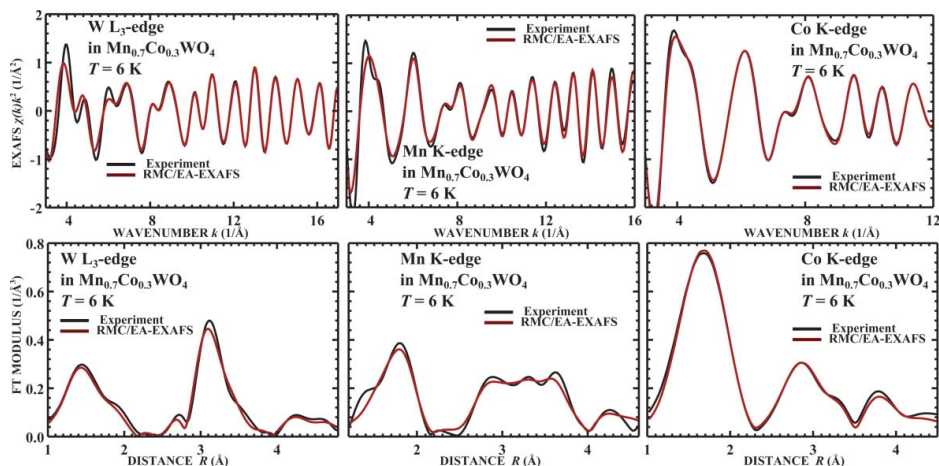
Figure 3. Comparison of the results of RMC/EA simulations (upper panels - EXAFS spectra, corresponding to the final structure model, bottom panels - moduli of their Fourier transforms (FT)) with the experimental W L_3-edge and Mn(Co) K-edges data for $Mn_{0.7}Co_{0.3}WO_4$ at $T = 6$ K.

well the W L_3-edge and Mn(Co) K-edges EXAFS spectra (Fig. 3) at all temperatures in the range from 6 K to 300 K.

Results and Discussion

The first coordination shell around W, Mn and Co atoms has been already analyzed in [3]. Therefore here we focus on the results, obtained for the nearest Mn(Co)-W atom pairs. There are 8 W atoms around each Mn(Co) atom, which are located at the distances between 3.0 Å and 4.5 Å and contribute strongly to the total EXAFS spectrum. Corresponding atomic radial distribution functions (RDFs), obtained from our RMC/EA simulations, are shown in Fig. 4. Upon increasing temperature no significant changes of the average Mn(Co)-W distances were observed. However, the widths of RDFs, characterized by the mean-square relative displacement (MSRD) factors, increase with temperature. This trend is shown in Fig. 5 and is analyzed in details below.

The RDF for Mn-W atom pairs has two pronounced maxima. The peak at about 3.75 Å corresponds to the four distant W atoms, located along the crystallographic *b*-axis from the absorbing Mn atom and represented in the scheme in Fig. 4 by atoms W_3 and W_4. In MnWO₄ this peak is very broad even at low temperatures. Corresponding MSRD values grow rapidly upon temperature increase, indicating that the interactions between Mn and $W_3(W_4)$ atoms are weak. These atom pairs are also sensitive towards the insertion of cobalt atoms: the corresponding Mn-W RDF peak in $Mn_{0.7}Co_{0.3}WO_4$ is significantly narrower than for pure MnWO₄.

The peak in the Mn-W RDF at about 3.5 Å (Fig. 5) corresponds to the four closest W atoms, located along the crystallographic *c*-axis from the absorbing Mn atom and represented in the scheme in Fig. 4 by atoms W_1 and W_2. In both investigated compounds this group of atoms shows smaller values of MSRD factors and their temperature dependence is also weaker. This indicates that the interatomic interaction between Mn and $W_1(W_2)$ atoms is stronger. This finding can be related with the rigidity of zigzag chains of edge-shared MnO₆ octahedra, located along the *c*-axis [14] and providing
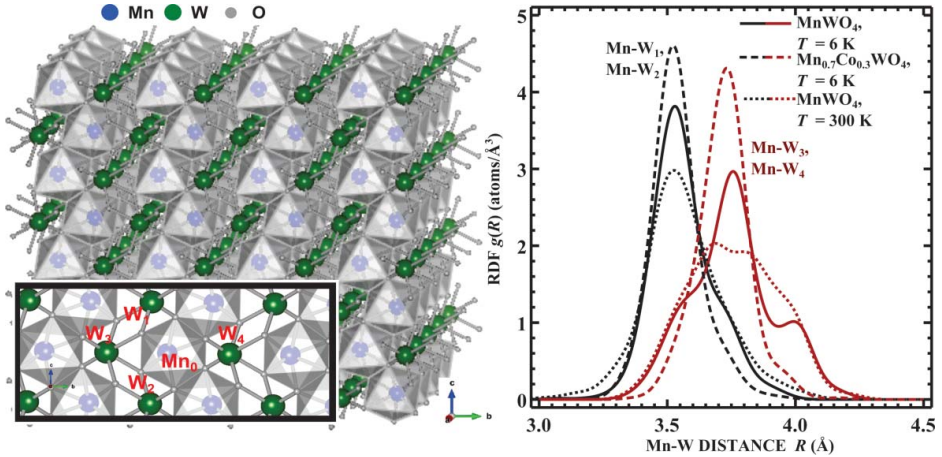
Figure 4. Crystal structure of $MnWO_4$ and RDFs for Mn-W atom pairs, obtained in RMC/EA simulations for $MnWO_4$ and $Mn_{0.7}Co_{0.3}WO_4$ at $T = 6$ K and for $MnWO_4$ at $T = 300$ K. The peak at about 3.75 Å corresponds to the distant W atoms (W_3 and W_4), located along the crystallographic b-axis from the absorbing Mn atom, while the peak at about 3.5 Å corresponds to the closest W atoms (W_1 and W_2), located along the crystallographic c-axis from the absorbing Mn atom.

the paths for the super-exchange interactions [15]. Also in this case, the insertion of cobalt atoms results in a decrease of the MSRD (Fig. 5) and the Mn-W RDF peak narrowing (Fig. 4).

Thus, these results support the conclusion derived by us in the previous work [3] that the presence of cobalt ions influences strongly the local environment around Mn atoms. The EXAFS data indicate clearly that upon manganese substitution by cobalt the tungstate structure becomes stiffer, and the distortion of the MnO_6 octahedra decreases. Such behaviour should directly affect both the Mn(Co)-O-Mn(Co) interchain magnetic interac-

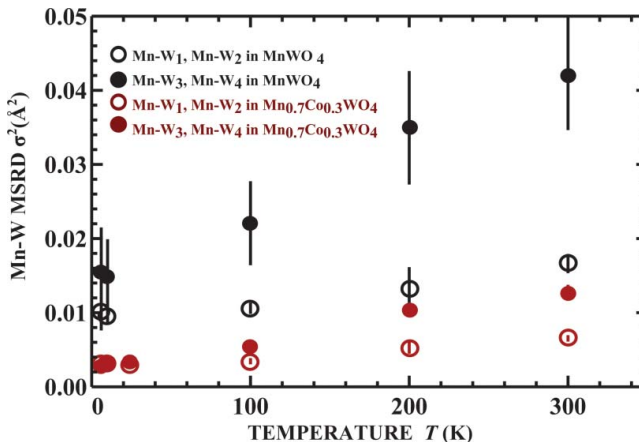**Figure 5.** Temperature dependence of the MSRD factors, obtained in RMC/EA simulations of $MnWO_4$ and $Mn_{0.7}Co_{0.3}WO_4$ for the Mn-W atom pairs along the crystallographic b- and c-axes.

tions along the *c*-axis and the intrachain magnetic interactions and is responsible for the increase of the Néel temperature at large cobalt content [2].

Conclusions

We employed wavelet analysis and RMC/EA simulations to interpret EXAFS spectra in crystalline $MnWO_4$ and $Mn_{0.7}Co_{0.3}WO_4$. It was shown that the high-frequency part of the W L_3 and Mn(Co) K-edge EXAFS spectra is dominated by contributions from the Mn(Co)-W atom pairs, and is sensitive to temperature and composition. Essential differences in the dynamics of the Mn-W atom pairs, located along the crystallographic *b*- and *c*-axes, were found. The interactions along the *c*-axis, corresponding to the direction of zigzag chains of edge-shared MnO_6 octahedra, appear to be stiffer.

Funding

References

1. O. Heyer, N. Hollmann, I. Klassen, S. Jodlauk, L. Bohaty, P. Becker, J. A. Mydosh, T. Lorenz, and D. Khomskii, A new multiferroic material: $MnWO_4$. *J. Phys.: Condens. Matter.* **18**, L471–L475 (2006).
2. Y. S. Song, J. H. Chung, J. M. S. Park, and Y. N. Choi: Stabilization of the elliptical spiral phase and the spin-flop transition in multiferroic $Mn_{1-x}Co_xWO_4$. *Phys. Rev. B.* **79**, 224415 (2009).
3. A. Kuzmin, A. Anspoks, A. Kalinko, and J. Timoshenko, Effect of cobalt doping on the local structure and dynamics of multiferroic $MnWO_4$ and $Mn_{0.7}Co_{0.3}WO_4$. *J. Phys.: Conf. Ser.* **430**, 012109 (2013).
4. J. Timoshenko, A. Kuzmin, J. Purans, EXAFS study of hydrogen intercalation into ReO_3 using the evolutionary algorithm. *J. Phys.: Condens. Matter.* **26**, 055401 (2014).
5. M. Munoz, P. Argoul, and F. Farges, Continuous Cauchy wavelet transform analyses of EXAFS spectra: a qualitative approach. *Am. Mineral.* **88**, 694–700 (2003).
6. J. Timoshenko, and A. Kuzmin, Wavelet data analysis of EXAFS spectra. *Comp. Phys. Commun.* **180**, 920–925 (2009).
7. K. Rickers, W. Drube, H. Schulte-Schrepping, E. Welter, U. Brüggmann, M. Herrmann, J. Heuer, H. Schulz-ritter et al., New XAFS facility for in-situ measurements at beamline C at HASYLAB. *AIP Conf. Proc.* **882**, 905–907 (2007).
8. V. L. Aksenov, M. V. Kovalchuk, A. Kuzmin, J. Purans, and S. I. Tyutyunnikov, Development of methods of EXAFS spectroscopy on synchrotron radiation beams, Crystallogr. *Rep.* **51**, 908–935 (2006).
9. R. L. McGreevy and L. Pusztai, Reverse Monte Carlo simulation: a new technique for the determination of disordered structures. *Mol. Simul.* **1**, 359–367 (1988).
10. J. Timoshenko, A. Kuzmin, and J. Purans, Reverse Monte Carlo modelling of thermal disorder in crystalline materials from EXAFS spectra. *Comp. Phys. Commun.* **183**, 1237–1245 (2012).
11. A. L. Ankudinov, B. Ravel, J. J. Rehr, and S. D. Conradson, Real-space multiple-scattering calculation and interpretation of x-ray-absorption near-edge structure. *Phys. Rev. B.* **58**, 7565–7576 (1998).

12. J. Timoshenko, A. Anspoks, A. Kalinko, and A. Kuzmin, Analysis of extended x-ray absorption fine structure data from copper tungstate by the reverse Monte Carlo method. *Phys. Scripta.* **89**, 044006 (2014).

13. F. Ye, S. Chi, J. A. Fernandez-Baca, H. Cao, K. C. Liang, Y. Wang, and C. W. Chu, Magnetic order and spin-flop transitions in the cobalt-doped multiferroic $Mn_{1-x}Co_xWO_4$. *Phys. Rev. B.* **86**, 094429 (2012).

14. M. Maczka, M. Ptak, K. Hermanowicz, A. Majchrowski, A. Pikul, and J. Hanuza, Lattice dynamics and temperature-dependent Raman and infrared studies of multiferroic $Mn_{0.85}Co_{0.15}WO_4$ and $Mn_{0.97}Fe_{0.03}WO_4$ crystals. *Phys. Rev. B.* **83**, 174439 (2011).

15. C. Tian, C. Lee, H. Xiang, Y. Zhang, C. Payen, S. Jobic, and M. H. Whangbo, Magnetic structure and ferroelectric polarization of $MnWO_4$ investigated by density functional calculations and classical spin analysis. *Phys. Rev. B.* **80**, 104426 (2009).